

## PROGRESS IN MODELING ARCS\*

Z. Insepov, J. Norem<sup>†</sup>, Argonne National Laboratory, Argonne, IL 60439, USA

A. Moretti, Fermilab, Batavia IL, 60510 USA

I. V. Morozov, G. E. Norman, Joint Institute of High Temperatures of RAS, Moscow, Russia

S. Mahalingam, S. Veitzer, Tech-X, Boulder, CO, 80303 USA

### Abstract

We are continuing to extend and simplify our understanding of vacuum arcs. We believe that all the breakdown phenomena we see (with and without B fields) can be explained by: 1) fracture due to electrostatic forces at surface crack junctions, 2) the development of a unipolar arc driven by the cavity electric field, and 3) cooling, and cracking of the surface after the event is finished. Recent progress includes the evaluation of non-Debye sheaths using molecular dynamics, studies of sheath driven instabilities, a model of degradation of gradient limits in strong B fields, analysis of the variety of arcs that can occur in cavities and their damage and further studies of breakdown triggers.

### INTRODUCTION

We numerically model all mechanisms crucial to arcing in the simplest and most general way. We ultimately disagree with most of the assumptions used to describe and understand dense vacuum arcs over the last 80 years.

Our picture of arc development is summarized in Fig. 1. Experimentally, two processes seem to control damage: 1) the formation and fracture of cracks and small structures, and, 2) the evolution and properties of unipolar arcs [1, 2]. Theoretically, we divide the arcing process itself into four elements: 1) mechanical failure (Coulomb explosion) of the surface producing fragments, 2) initial ionization of the fragments by field emission (FE) currents, 3) exponential density growth of the unipolar arc, and, 4) surface damage. Many of the details of these mechanisms have been described in earlier papers. We describe detailed calculations on the non-ideal plasma sheath, which seems to contain the essential mechanisms of surface damage by plasmas[3]. Recent progress has also included a better understanding of the production of field enhancements required to produce the initial fracture that triggers breakdown, particularly in magnetic fields. We have continued to study these surface damage mechanisms under a variety of conditions.

These arcs act as virtual cathodes and produce currents that short the cavity fields. Once an arc starts, the surface electric field, and field emission increase, increasing ionization of neutrals, causing an increase in the plasma density. The density increase decreases the Debye length and causes an increase in the surface electric field, producing

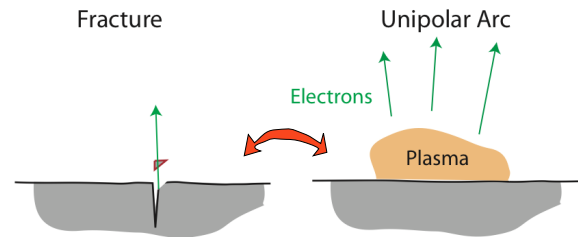


Figure 1: The arc process is controlled by: 1) fracture of high field areas at crack junctions and, 2) the evolution of the unipolar arc, driven by sheath parameters.

and exponential increase in both the electric field and the density with time, roughly described by the blue arrow in Fig. 2. PIC simulations of the unipolar arc model for vacuum arcs relevant to rf cavity breakdown [4] show that the density of plasma formed above the field emitting asperities can be as high as  $10^{26} \text{ m}^{-3}$ . The temperature of such plasma is low, in the range of 1 – 10 eV.

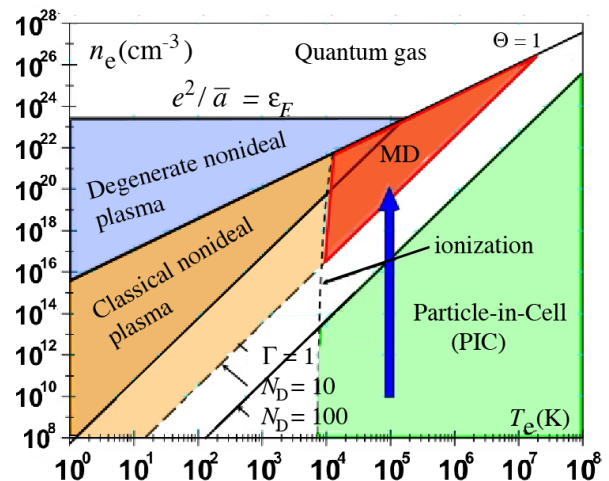


Figure 2: The plasma parameter space during breakdown, showing applicable modeling techniques.

At these high densities the Debye screening length,  $\lambda_D = \sqrt{\epsilon_0 k_B T / n_e e^2}$ , becomes smaller than the mean inter-particle distance, causing the number of particles in the Debye sphere,  $N_D = 4\pi n_e \lambda_D^3 / 3$ , to become less than unity. As the density increases modeling with a PIC code becomes less precise because the interactions are no longer two body scattering. There is a general lack of experience with modeling non-ideal plasmas and with the density lim-

\*The submitted manuscript has been created by UChicago Argonne, LLC, Operator of Argonne National Laboratory ("Argonne"). Argonne, a U.S. Department of Energy Office of Science laboratory, is operated under Contract No. DE-AC02-06CH11357. Work supported by Office of High Energy Physics, USDOE.

<sup>†</sup>norem@anl.gov

itations of PIC codes. We find that an approximate picture of the domain of applicability of PIC and MD codes is shown in Fig 2. The degree of non-ideality of the plasma is measured by the ratio  $\Gamma$  of the potential energy divided by kinetic energy of the plasma.

Equilibrium and non-equilibrium non-ideal plasmas have been studied extensively by MD in the past several decades [3]. Nevertheless there are few studies of the spatially inhomogeneous systems such as the plasma sheath. Ref [3] gives the first results for MD simulations of the non-ideal plasma sheath near a metallic surface.

### SHEATH PARAMETERS

We consider a two-component fully ionized electron-ion plasma. In the present work the simulations are restricted to the singly ionized, copper plasma with  $Z = 1$ .

The procedure is: 1) creation of a set of initial states of ions and electrons, 2) freezing the ion motion and allowing the electrons to go to the wall until this motion is balanced by electrostatic forces, and, 3) averaging the results obtained with different initial states. The electron-electron and ion-ion interactions are given by the Coulomb potential. For electrons and ions it is modified at short distances to account for quantum effects. The equation below assumes a Gaussian wave function for an electron

$$V_{ei}(r) = \frac{Ze^2}{4\pi\epsilon_0 r} \text{erf}\left(\frac{r}{r_0}\right),$$

where the  $r_0$  parameter that equals to 0.21 nm in our case to match the ionization energy for copper at  $r = 0$ :  $U(0) = -7.73$  eV. More detailed information is available in Ref [3, 5]. The results are weakly dependent on the short distance part of the potential as the change of the  $U(0)$  value from 7.73 eV to 5.1 eV does not change the results within simulation accuracy. Neutral atoms are not taken into account, which can affect relaxation times at relatively low plasma densities when the density of neutrals is high enough. It should not, however, affect the stationary distribution of charges.

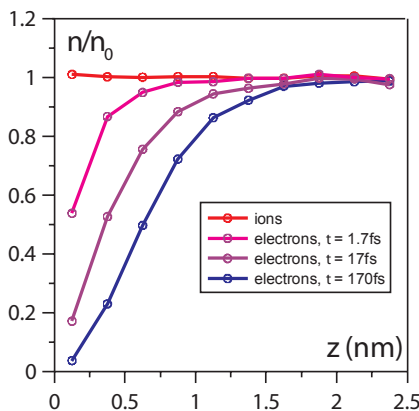


Figure 3: Sheath evolution at  $10^{23} \text{ m}^{-3}$ .

The formation of the sheath takes about 200 fs. The density profiles obtained after the relaxation are shown in

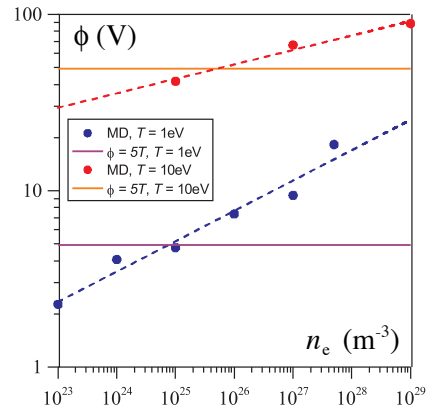


Figure 4: Sheath parameters as a function of electron temperature and density.

Fig.3. The electron deficit defines the plasma sheath. This technique can be used to evaluate the material dependence of the plasma sheath and burn voltage of the arc. Fig. 4 shows the parameters of the sheath.

The exponential increase in density and surface field seen in PIC codes will be shorted out by field emission at  $\sim 3$  GV/m. This value of the maximum field corresponds to FE current densities of  $i_{shorting} = \epsilon_0 E / \delta t \sim 20 \text{ MA/m}^2$ , with  $\delta t = 1$  ns, the approximate plasma growth time. We anticipate this will produce oscillations in the 100 - 500 MHz range, and see these oscillations [3]. When multiplied by the area of the melted spot seen in 805 MHz cavities, we determine that the shorting current from this mechanism would be about 4 A, equal to the value seen in x ray measurements from the MAP 805 MHz pillbox cavity [2].

Arcs in other cavities (for example CLIC), where shorting currents of hundreds of Amps are required, would be constrained the same current density limits, implying that the arcs must be much larger, perhaps filling the cavity or at least a few cells. This is consistent with SEM images showing large melted areas ( $\sim \text{cm}^2$ ) and spinodal decomposition, see Fig. 5 [6].

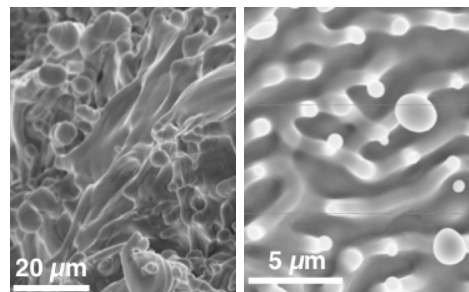


Figure 5: Images from large area arcing in CLIC structures. The image on the left shows spinodal decomposition [6].

## EFFECTS OF B FIELDS

Recent experimental data show the effects of magnetic fields on surface damage. Parallel electric and magnetic fields confine the shorting currents to a small area on the far side of the cavity producing small round arcs and melted areas. When these arcs cool and contract, they produce small intensely cracked central regions surrounded by large smooth areas, see Fig 6. For both the  $B = 0$  and  $B = 3$  T cases, the integrated width of these cracks is about 2 % of the diameter of the melted area, *i.e.*,  $\Delta x/x = \alpha \Delta T \sim 2\%$ , where  $\Delta T$  is  $1000^\circ$  C and  $\alpha$  is the linear expansion coefficient. In the  $B = 3$  T case, the cracks were densely confined in a region about  $10 \mu\text{m}$  in diameter. We assume that a higher density of cracks produces more crack junctions, giving more possible breakdown sites and lower maximum fields.

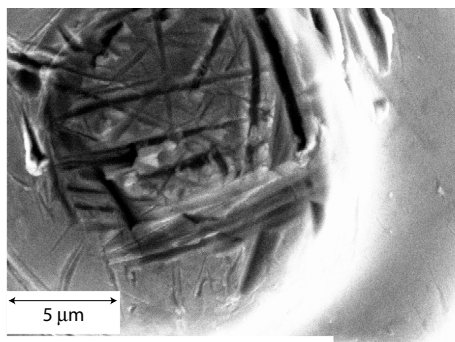


Figure 6: At  $B = 3$  T, cracking is confined to the  $10 \mu\text{m}$  diameter center of a  $500 \mu\text{m}$  diameter melt spot, producing more crack junctions (*i.e.* breakdown sites). Mirror images of the mm scale damage patterns appear at both ends of cavities when the damage occurs in magnetic fields.

## GAS FILLED CAVITIES

High pressure gas has been proposed as a way of combining the absorber required for muon cooling with the arc suppression features of  $\text{SF}_6$  [7]. Recent experimental results have been described in Ref [8]. The arc model described above explains arc suppression due to high pressure gas as a low energy attenuation of the field emitted electrons before they are able to ionize fragments broken off of the surface by tensile stresses. An early calculation, Ref [7], showed that this attenuation is effective in preventing breakdown by slowing down field emitted electrons before they can ionize fragments, but at higher fields, the surface can break down normally. Gas filled cavities are sensitive to ionization due to muons and impurities in the beam, making the gas conductive. Above 1 keV energy, the retarding force due to  $dE/dx$  scattering of ionization electrons (delta rays) is less than the applied accelerating field, and these electrons would run away, further loading the cavity, this loading is dependent on the intensity of charged particles and the cavity length. The number of high energy secondaries produced per electron in high pressure hydrogen has been calculated by Seitz since this

mechanism is similar to the formation of bubbles in hydrogen bubble chambers with comparable density [9].

## CONCLUSIONS

Our numerical results imply that breakdown events are triggered by mechanical failure at high field regions of surface crack junctions. We find that the arc behavior is dominated by avalanche processes at the surface that produce a non-ideal non-Debye plasma that seems to be limited by field emitted shorting currents at about 3 GV/m (20 MA/m current density). These processes should be time, material and structure dependent. The model can also consider gas filled cavities. These methods extend the model to other arc behaviors, in tokamaks, micrometeorites and laser produced unipolar arcs.

Our numerical results do not, however, support the conventional wisdom in arcing studies. Fowler-Nordheim plots seem unnecessarily indirect and confusing. Single structures with significant field enhancements ( $\beta$ s) are not found in cavities [2, 3, 4, 5]. Ohmic heating of solid material seems too slow to be significant, and we find that the current densities and structures (both solid and liquid) are too small to generate significant heating.

## ACKNOWLEDGMENTS

We thank the staff of the Accelerator and Technical Divisions at Fermilab and the Muon Accelerator Program (MAP) for supporting and maintaining the MAP experimental program in the MTA experimental area. D. Bowring, LBNL, provided some of the samples measured. The work at Argonne is supported by the U.S. Department of Energy Office of High Energy Physics under Contract No. DE-AC02-06CH11357. I. Morozov acknowledges the support by the Programs of Fundamental Research of RAS Nos. 2, 13 and 14. Computations were performed on clusters MIPT-60 and K100 (KIAM RAS).

## REFERENCES

- [1] Z. Insepov, J. Norem, S. Veitzer, S. Mahalingam, Proceedings of RF2011, June 1-3, Newport R. I., IAP Conference Proceedings 1406, Melville New York (2011), arXiv:1108.0861.
- [2] Z. Insepov, J. Norem, Th. Proslie, A. Moretti D. Huang, S. Mahalingam, S. Veitzer; arXiv:1003.1736 (2010).
- [3] I. V. Morozov, G. E. Norman, Z. Insepov, J. Norem, Phys. Rev. STAB **15** 053501 (2012).
- [4] F.R. Schwirzke; IEEE T. Plasma Sci. **19**, No. 5, 690 (1991).
- [5] A. Anders, *Cathodic Arcs, From Fractal Spots to Energetic Condensation*, Springer, New York (2008), Chapter 3
- [6] G. Arnau Izquierdo talk at <http://indico.cern.ch/conferenceDisplay.py?confId=33140>.
- [7] Private Communication, R. Johnson, (2004).
- [8] K. Yonehara, M. Jana, M. Leonova, A. Moretti, M. Popovic, A. Tollestrup, M. Chung, B. Freemire, Y. Torun, R. Johnson, M. Collura, "Investigation of Breakdown Plasma in High-pressure Hydrogen Gas-filled RF Cavity". MOPPC036, these proceedings.
- [9] F. Seitz, Physics of Fluids, **1**, 2 (1958).